HOSTED BY

ELSEVIER

CrossMark

Available online at www.sciencedirect.com

ScienceDirect

Progress in Natural Science: Materials International 24 (2014) 479–485

Progress in Natural Science Materials International

www.elsevier.com/locate/pnsmi
www.sciencedirect.com

Original Research

Doping inorganic ions to regulate bioactivity of Ca–P coating on bioabsorbable high purity magnesium

Hongliu Wu[a], Ruopeng Zhang[a], Xiao Li[a], Jiahua Ni[a], Changli Zhao[a], Yang Song[b], Jiawei Wang[a], Shaoxiang Zhang[c], Yufeng Zheng[d], Xiaonong Zhang[a,c,*]

[a]*State Key Laboratory of Metal Matrix Composites, School of Materials Science and Engineering, Shanghai Jiao Tong University, Shanghai 200240, China*
[b]*Department of Mechanical Engineering, The University of Hong Kong, Hong Kong, China*
[c]*Suzhou Origin Medical Technology Co. Ltd., Jiangsu 215513, China*
[d]*State Key Laboratory for Turbulence and Complex System, Department of Materials Science and Engineering, College of Engineering, Peking University, Beijing 100871, China*

Received 2 July 2014; accepted 1 September 2014
Available online 18 October 2014

Abstract

Performance of biomaterials was strongly affected by their surface properties and could be designed artificially to meet specific biomedical requirements. In this study, F^- (F), SiO_4^{2-} (Si), or HCO_3^- (C)-doped Ca–P coatings were fabricated by biomimetic deposition on the surface of biodegradable high-purity magnesium (HP Mg). The crystalline phases, morphologies and compositions of Ca–P coatings had been characterized by X-ray diffraction (XRD), scanning electron microscopy (SEM) and energy-dispersive spectroscopy (EDS). The biomineralization and corrosion resistance of doped Ca–P coatings had also been investigated. The results showed that the Ca–P coating with or without doped elements mainly contained the plate-like dicalcium phosphate dehydrate (DCPD) phase. The doped F, Si, or C changed the surface morphology of Ca–P coatings after mineralization. Doped F enhanced the mineralization of Ca–P coating, and doped Si retarded the mineralization of Ca–P coating. However, H_2 evolution of HP Mg discs with different Ca–P coatings was close to 0.4–0.7 ml/cm^2 after two-week immersion. That meant that the corrosion resistance of the Ca–P coatings with different or without doped elements did not change significantly.

Keywords: Calcium phosphate coating; Adjustable bioactivity; Magnesium; Biomimetic deposition; In vitro

1. Introduction

Recently, the bioactive and bioabsorbable magnesium alloys have been extensively investigated as implants for orthopedic and cardiovascular applications [1–5]. This was because they were considered capable of meeting the required biocompatibility at different implantation positions. For instance, magnesium alloys used as biological bone substitution materials could promote the precipitation of calcium phosphate and consequently stimulated the new bone growth [6]. However, some studies also suggested that the calcium phosphate deposition could cause the unwanted soft tissue calcification, thus increasing the risk of myocardial infarction as the cardiovascular stents [7,8].

Many efforts have been made to smelt magnesium alloys with different compositions [9–11], but the enhancement of the biological performance of magnesium alloys by smelting was rather limited due to the high degradation rate. However, it has been reported that the biological performance of magnesium alloys could be significantly improved by surface modification [12–14]. For example, the hydroxyapatite coating on Mg alloys has been proved to effectively reduce the degradation rates of Mg alloys [15–18] and dramatically enhance the connection between the implants and the fractured bones [17].

The in vivo performance of magnesium alloys depended strongly on their surface properties, and thus it was necessary

*Corresponding author at: State Key Laboratory of Metal Matrix Composites, School of Materials Science and Engineering, Shanghai Jiao Tong University, Shanghai 200240, China. Tel./fax: +86 21 3420 2759.
E-mail address: xnzhang@sjtu.edu.cn (X. Zhang).
Peer review under responsibility of Chinese Materials Research Society.

http://dx.doi.org/10.1016/j.pnsc.2014.08.004
1002-0071/

to prepare adjustable bioactive coatings on the surface to serve different purposes of implantation [19]. According to the previous research [20], the Ca–P coating has different ions which can be replaced by other ions. In the present work, the Ca–P coatings with different doping ions (Si, F, and C) were fabricated by biomimetic deposition on the surface of HP Mg. The bioactivity, morphology and corrosion resistance of Ca–P coatings with different doping ions were investigated.

2. Experimental

2.1. Fabrication of Ca–P coating

HP Mg discs (∅11.3 × 2 mm, ≥ 99.99% purity) were used as the substrate for biomimetric deposition. The discs were ground up to 1200# SiC paper to obtain the same surface roughness [21], and then ultrasonically cleaned in ethanol and dried in air.

Four groups of feeding solutions with different additives were used to prepare coatings on the surface of the HP Mg discs (see Table 1). The solution consisting of 0.042 M $CaCl_2$ and 0.025 M NaH_2PO_4 was used as the control group. The others added extra 0.001 M Na_2SiO_3, 0.002 M NaF, 0.005 M $NaHCO_3$, respectively. For each group of feeding solutions, three HP Mg discs were immersed simultaneously in 250 ml solution for 30 min for preparation of coatings.

2.2. Biomineralization test

According to Marc Borhner's protocol [18], all HP Mg discs with the Ca–P coatings obtained by biomimetic deposition were immersed into the SBF-JL2 solution for 24 h at 37 °C under the atmosphere of 5 vol% CO_2 for the measurement of Ca/P ratio of coatings. The ratio of liquid volume to the surface area of each sample was set to 200 ml/cm^2.

2.3. Corrosion resistance test

Four groups of discs with Ca–P coatings were immersed into the modified simulated body fluid (m-SBF) for the measurement of corrosion resistance. Each sample was immersed into 100 ml m-SBF and the immersion was repeated three times for each group of coatings. The m-SBF solution was prepared according to the procedure described by Oyane et al. [22] and was added with HEPES (4-(2-hydroxyethyl)-1-piperazine ethanesulfonic acid) as buffer. Hydrogen release and pH value were recorded in different periods during 2 week immersion to analyze the corrosion resistance of different Ca–P coatings. In this section, the corrosion resistance of the bare Mg disc was also measured.

Table 1
The composition and concentration of different feeding solutions.

	$CaCl_2$ (M)	NaH_2PO_4 (M)	Na_2SiO_3 (M)	NaF (M)	$NaHCO_3$ (M)
Control group	0.042	0.025			
Ca–P–Si group	0.042	0.025	0.001		
Ca–P–F group	0.042	0.025		0.002	
Ca–P–C group	0.042	0.025			0.005

2.4. Characterization

All samples were rinsed with distilled water and dried in the air after immersion. The surface morphologies of the Ca–P coatings before and after immersion were observed by scanning electron microscope with Energy Dispersive X-ray Spectrometry (SEM/EDS, FEI Quanta FEG 250). The crystallized phases of the coatings on HP Mg discs were detected by the X-ray diffraction (XRD, Rigaku, D/MAX255).

3. Results and discussion

3.1. Morphology and composition of Ca–P coating

Fig. 1 is the XRD pattern of the Ca–P coatings on the surface of HP Mg discs obtained in four feeding solutions after 30 min immersion. For all the four groups, the typical

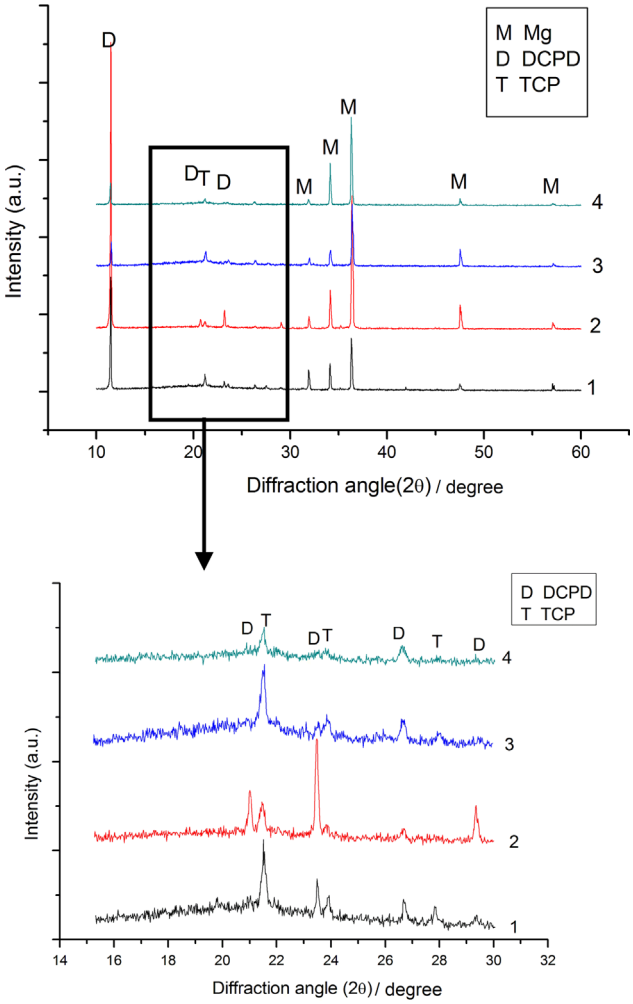

Fig. 1. XRD of the coatings on the surface of HP Mg discs after 30 min immersion. (1) Control group; (2) Ca–P–Si group; (3) Ca–P–F group; (4) and Ca–P–C group.

crystallized peaks of brushite (DCPD, $CaHPO_4 \cdot 2H_2O$) appeared at $2\theta = 11^\circ$, 21°, and 29.5°, respectively. The weak peak at $2\theta = 23.5^\circ$ indicated that there were some tricalcium phosphate (TCP, $Ca_3(PO_4)_2 \cdot xH_2O$). Moreover, the diffraction peaks of Mg and MgO were obvious.

Fig. 2 showed the surface morphologies of the four Ca–P coatings. The coating obtained in the control group was loose, with polygonal plate-like structures on a scale of 40–60 μm (Fig. 2a). The coating in the Ca–P–Si group consisted of clusters composed of polygonal plate-like substance on a scale of 20–30 μm, which was smaller than those of the control group. Under the clusters, there existed larger plate-like crystals with size of 40–50 μm (Fig. 2b). For the Ca–P–F group (Fig. 2c), the coating was composed of huge and dense plate-like crystals, of which structure was similar to the control group. A few globules were spread on the plate-like structure (Fig. 2c). In Fig. 2d, the plate-like crystals with size of 30–40 μm laid loosely on the surface of Ca–P–C group, meanwhile, the larger plate-like crystals as shown in Fig. 2a existed on the surface. Combined with the XRD pattern, the plate-like structure was identified to be DCPD phase.

In this experiment, HP Mg once immersed in the feeding solutions, magnesium provided free electrons for the reductive reactions of $H_2PO_4^-$ derived from feeding solution, which leaded to the formation of $H_2PO_4^{2-}$ and PO_4^{3-} $H_2PO_4^{2-}$ and PO_4^{3-} bonded with Ca^{2+}. Meanwhile, SiO_3^{2-}, F^-, HCO_3^- bonded with Ca^{2+} to form the Si, F or C-doped Ca–P minerals and then deposited on the surface of Mg discs due to the limit of solubility. Ultimately, the coatings with different doped ions were obtained by adding SiO_3^{2-}, F^- and HCO_3^{2-} into the feeding solution. As observed in Fig. 2, it was obvious that the size of DCPD phases in the Ca–P–F group was the smallest, and the next was the Ca–P–C case. From the above results, it was speculated that the existence of Si and C could hinder the growth of large crystals of DCPD flakes compared with the control group and the Ca–P–F group. In addition, it has been proved that the DCPD phase in the coatings had bioactivity [23], and thus the different dopants in Ca–P coatings could lead to different bioactivity.

3.2. Biomineralization of Ca–P coating

To verify the above assumption, the as-prepared coated samples were immersed into the SBF-JL2 solution for 24 h, allowing the transition of the coating precursor of DCPD and TCP in a simulated physiological environment. Table 2 showed the Ca/P ratio of the coatings before and after immersion in SBF-JL2 detected by EDS. The EDS results of the four groups of Ca–P coatings before and after the immersion showed the same elements. Before immersion, the difference of Ca/P ratio was negligible, but after immersion, it was obvious that the Ca/P ratio increased for all groups. For

Table 2
Calcium and phosphate ions' molar ratio of the coating on HP Mg before and after immersion in SBF-JL2.

Ca/P	As-precipitated coatings	After immersion in SBF-JL2
Control group	0.92	1.17
Ca–P–Si group	0.94	1.00
Ca–P–F group	0.95	1.46
Ca–P–C group	0.91	1.15

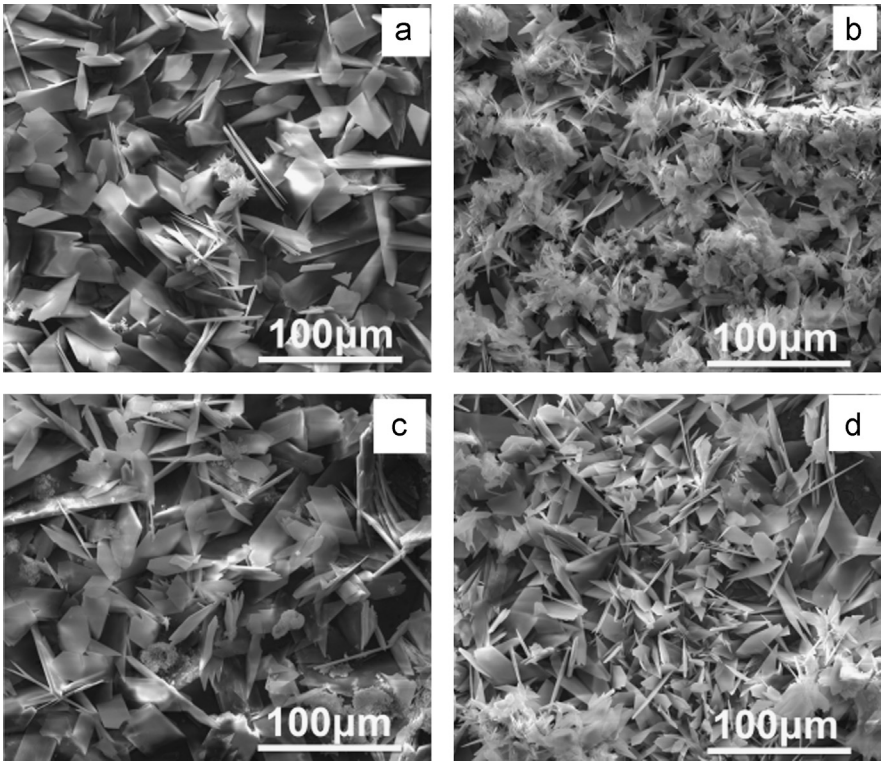

Fig. 2. SEM images of the Ca–P coating on HP Mg after pretreatment. (a) Control group; (b) Ca–P–Si group; (c) Ca–P–F group; and (d) Ca–P–C group.

the Ca–P–F group, its Ca/P ratio significantly increased from 0.95 to 1.46, and the largest range indicated the best mineralization efficiency of the coatings in the feeding solution with the aid of F. The Ca/P ratio of the control group and the Ca–P–C group rose from 0.92 to 1.17 and from 0.91 to 1.15, respectively. For the Ca–P–Si group, the Ca/P ratio had limited increase from 0.94 to 1.00, which illustrated that the mineralization degree was the lowest and also showed Si hinder the mineralization of Ca–P coating.

Fig. 3 showed the XRD patterns of the Ca–P coatings after 24 h immersion into SBF-JL2. It was obvious that the intensity of the diffraction peak of DCPD and TCP at $2\theta = 23.4^\circ$ (Fig. 3) decayed dramatically compared with Fig. 1, especially for the Ca–P–F group and the Ca–P–C group, which illustrated fast conversion of the DCPD and TCP phases happened with the aid of F and C. However, the intensity of DCPD peak at $2\theta = 11^\circ$ did not change greatly.

Fig. 4 showed the surface SEM images of the Ca–P coatings after 24 h immersion into SBF-JL2. For the control group, a tangle containing flake-like phase with a size of 20–30 μm and cluster with a size of 15 μm were covered on the surface

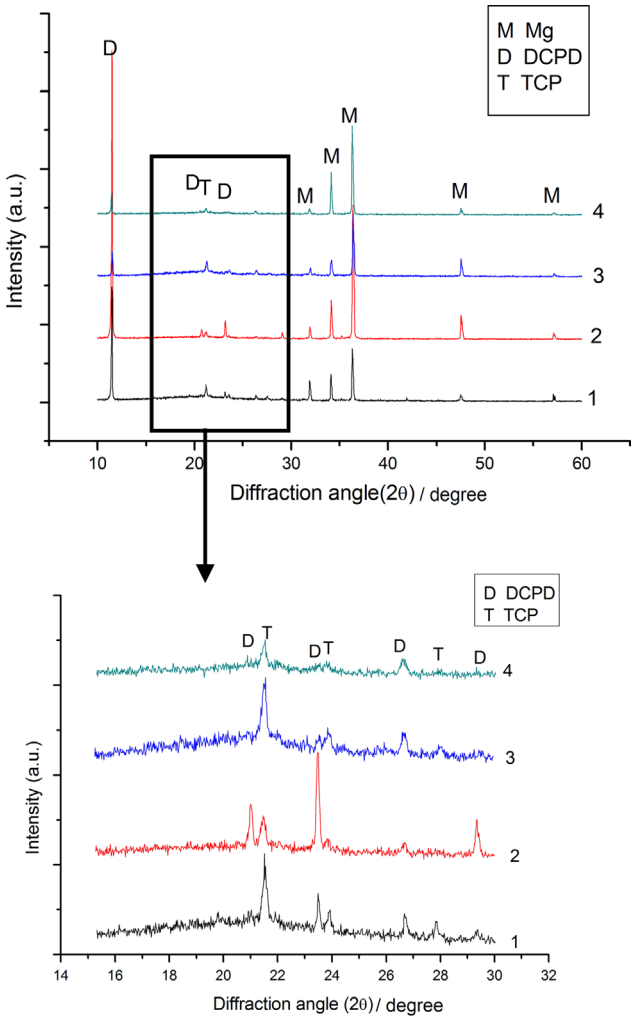

Fig. 3. XRD of the coatings on HP Mg after post-treated by SBF-JL2 for 24 h. (1) Control group; (2) Ca–P–Si group; (3) Ca–P–F group; and (4) Ca–P–C group.

(Fig. 4a). The flake-like phase was 30–50 μm on the surface of Ca–P–Si group (Fig. 4b). The coating of Ca–P–F group had clumped, and some cracks with a few micrometers width existed simultaneously (Fig. 4c). The mixture of strip-shape substance and cluster was appeared on the surface of Ca–P–C group (Fig. 4d). It was obvious that the surface morphologies of four Ca–P coatings after 24 h immersion into SBF-JL2 showed clear variations compared with those in Fig. 2. The notable change was the flake-like phase structure on the surfaces of control group, Ca–P–F group and Ca–P–C group disappeared. On the contrary, the flake-like phase structure dominated in the Ca–P–Si group. From the disappearance of DCPD phase and the significant decrease of DCPD peaks' intensity of Ca–P–F group and Ca–P–C group after immersion into SBF-JL2, it was concluded that the addition of F and C into the coatings resulted in a faster dissolution of DCPD phase.

Bioactivity of the coatings relied on their compositions and initial phase structures. From the results shown in Table 2, Figs. 3 and 4, the bioactivities of Ca–P coatings could be adjusted by adding other functional elements into coatings for some specific purposes at different implantation sites. As the bone-substitution materials, a strong connection between the materials and the fractured bones was necessary, hence, the bioactive Ca–P–F coating prepared in this work had the important advantage of enhancing the connection between coating and bone due to the fast mineralization rate. In comparison, the bioactive Ca–P–Si coating with low mineralization rate seemed more suitable for soft tissue or implantation site without fast calcification.

3.3. Corrosion resistance of Ca–P coating

The corrosion resistance of Ca–P coating was characterized by H_2 release and pH value of residual m-SBF recorded at different immersion periods (see Fig. 5). Fig. 5a shows the change trend of H_2 emission of all groups during the first week immersion (the H_2 evolution did not change during the second week, and thus omitted). The bare HP Mg showed the highest H_2 release up to 4.5 ml/cm^2 due to fast degradation. The H_2 evolution of the control group and the Ca–P–F group was close to 0.7 ml/cm^2, while the Ca–P– group and Ca—C group were as low as 0.4 ml/cm^2, which demonstrated that the fully Ca–P coating can significantly decrease the degradation rate of Mg alloy substrate. Although the degradation rate of bare disc was far higher than that of the Ca–P coated discs, all H_2 emission curves showed the same change trend during one week immersion. The H_2 evolution rate stayed at the highest level during the first 12 h, and then gradually decreased until the steady stage. The pH value of all groups of samples gradually increased during two-week immersion and still showed the same change trend (Fig. 5b). The bare disc group showed the highest pH increase up to 8.1. The lowest pH increase was the Ca–P–C group and the control group. These data suggested that the Ca–P–C group performed the best corrosion resistance among the four groups of coatings.

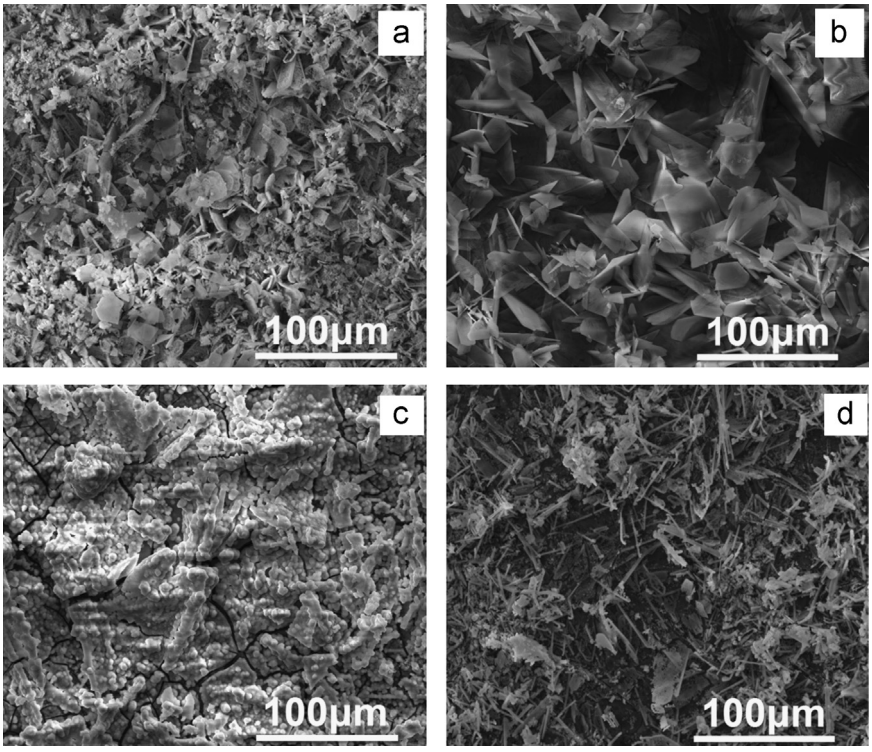

Fig. 4. SEM images of the coating structure on HP Mg after post-treated by SBF-JL2 for 24 h. (a) Control group; (b) Ca–P–Si group; (c) Ca–P–F group; and (d) Ca–P–C group.

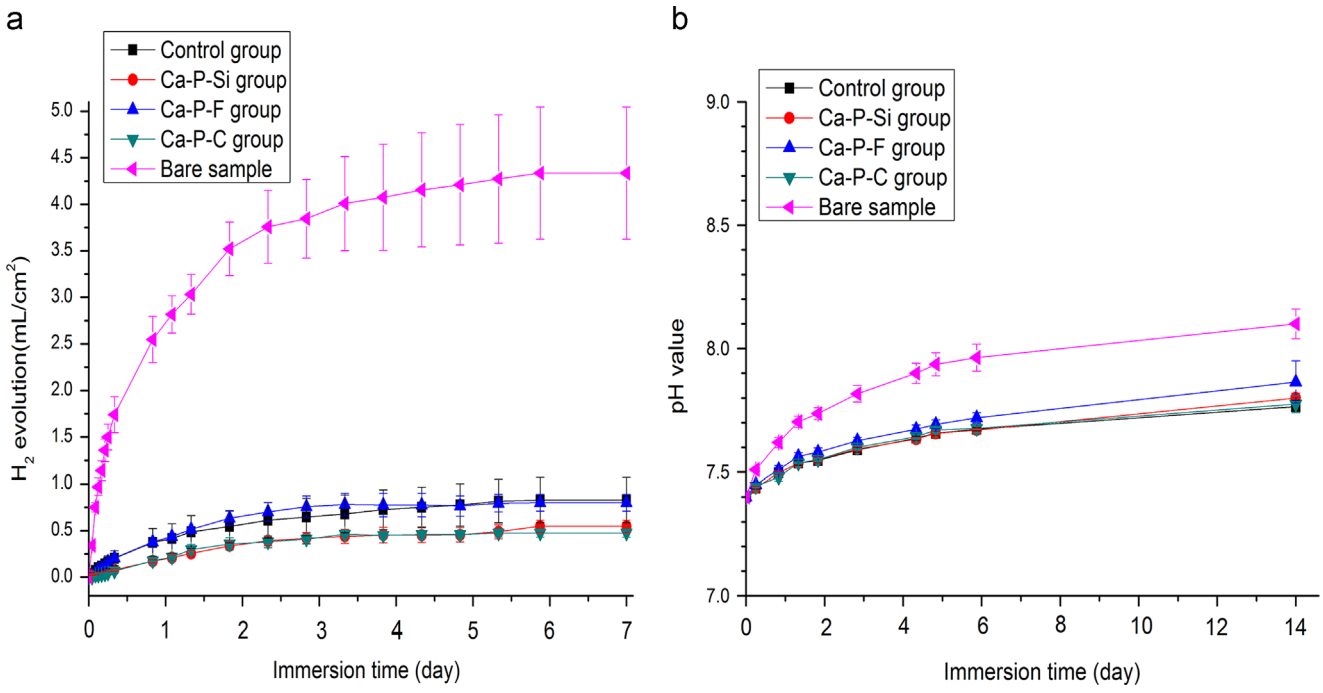

Fig. 5. Hydrogen evolution (a) and pH value (b) for HP Mg with different coatings immersed in m-SBF at 37 °C.

The morphologies of HP Mg with or without Ca–P coatings after 2 weeks immersion in m-SBF are shown in Fig. 6. For the control group (Fig. 6a), the plate-like DCPD crystals before immersion (Fig. 2a) became a dominant river-like structure. The remained plate-like DCPD with a size of 30–40 μm (white arrow in Fig. 6b) was on the Ca–P–Si group. Moreover, a small area of the HP Mg substrate was uncovered, as shown in the highlighted area in Fig. 6b. Obviously, the precipitates with a cotton-like structure (white arrow in Fig. 6c) were distributed on the surface of Ca–P–F group except the residual plate-like DCPD (Fig. 6c). The surface morphology of Ca–P–C group was similar to that of the control group, but there was a small

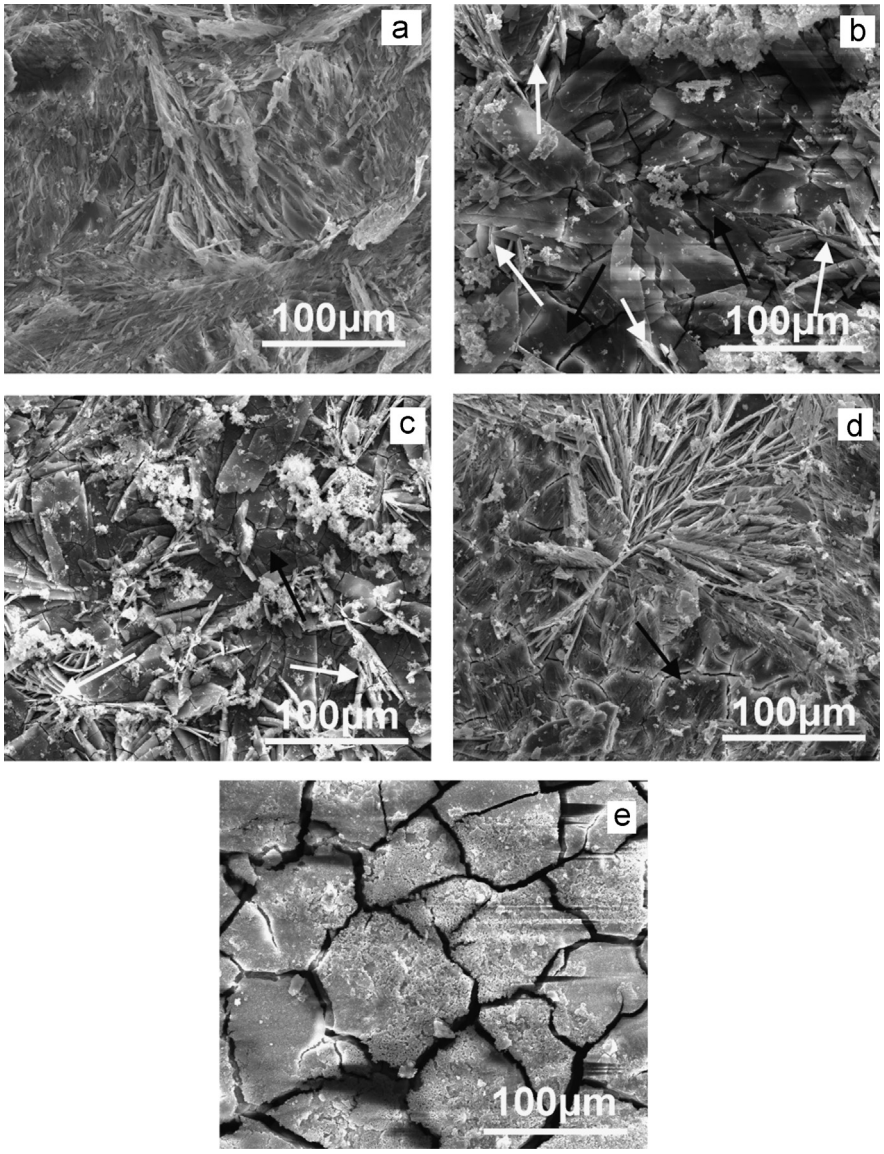

Fig. 6. SEM images of the surface of coating on HP Mg discs after immersion in m-SBF for 2 weeks. (a) Control group; (b) Ca–P–Si group; (c) Ca–P–F group; (d) Ca–P–C group; (e) bare disc sample. Black arrow: base of HP Mg. White arrow: plate-like structure.

area of the HP Mg substrate exposed (shown in the highlighted area in Fig. 6b). On the contrary, massive corrosion products were observed on the bare HP Mg disc with cracks distributed on the surface (Fig. 6e). Although Ca–P coatings improved the corrosion resistance of HP Mg, the different additives (Si, F, and C) in Ca–P coatings did not significantly change the corrosion resistance of the coatings, and just changed the surface morphology and compositions of coatings.

4. Conclusions

As a summary, the Ca–P coating with or without doped ions mainly contained the plate-like DCPD phase. F could enhance the mineralization of Ca–P coating, and Si hindered the mineralization. Meanwhile, F and C leaded to the fast conversion of coating precursors of DCPD and TCP. However, H_2 evolution varied from 0.7 ml/cm^2 for Ca–P–F group to 0.4 ml/cm^2 for Ca–P–Si and Ca–P–C group after one week immersion, indicating doped with Si, F, or C did not change so much on the corrosion resistance of Ca–P coatings.

Acknowledgments

The authors are grateful for supports from the National Natural Science Foundation of China (No. 51271117), the National Basic Research Program of China (973 Program, No. 2012CB619102), the Jiangsu Science Foundation for Young Scholars (Grant no. BK2012206) and the Shanghai Committee of Science and Technology, China (No. 14441901800).

References

[1] J. Lévesque, H. Hermawan, D. Dubé, D. Mantovani, Acta Biomater. 4 (2008) 284–295.

[2] M.P. Staiger, A.M. Pietak, J. Huadmai, G. Dias, Biomaterials 27 (2006) 1728–1734.
[3] S. Zhang, X. Zhang, C. Zhao, J. Li, Y. Song, C. Xie, H. Tao, Y. Zhang, Y. He, Y. Jiang, Y. Bian, Acta Biomater. 6 (2010) 626–640.
[4] J. Nagels, M. Stokdijk, P.M. Rozing, J. Shoulder Elb. Surg. 12 (2003) 35–39.
[5] C.Y. Zhang, R.C. Zeng, R.S. Chen, C.L. Liu, J.C. Gao, T. Nonferr, Met. Soc. 20 (2010) s655–s659.
[6] H. Zreiqat, C.R. Howlett, A. Zannettino, P. Evans, G. Schulze-Tanzil, C. Knabe, M. Shakibaei, J. Biomed. Mater. Res. 62 (2002) 175–184.
[7] C.M. Giachelli, Kidney Int. 75 (2009) 890–897.
[8] W.L. Lau, M.H. Festing, C.M. Giachelli, Thromb. Haemost. 104 (2010) 464–470.
[9] F. Witte, H. Ulrich, M. Rudert, E. Willbold, J. Biomed. Mater. Res. A 81 (2007) 748–756.
[10] F. Witte, V. Kaese, H. Haferkamp, E. Switzer, A. Meyer-Lindenberg, C.J. Wirth, H. Windhagen, Biomaterials 26 (2005) 3557–3563.
[11] B. Heublein, R. Rohde, V. Kaese, M. Niemeyer, W. Hartung, A. Haverich, Heart 89 (2003) 651–656.
[12] E.C. Meng, S.K. Guan, H.X. Wang, L.G. Wang, S.J. Zhu, J.H. Hu, C.X. Ren, J.H. Gao, Y.S. Feng, Appl. Surf. Sci. 257 (2011) 4811–4816.
[13] H. Wang, S. Zhu, L. Wang, Y. Feng, X. Ma, S. Guan, Appl. Surf. Sci. 307 (2014) 92–100.
[14] N. Li, Y.D. Li, Y.B. Wang, M. Li, Y. Cheng, Y.H. Wu, Y.F. Zheng, Surf. Interface Anal. 45 (2013) 1217–1222.
[15] H. Wang, C. Zhao, Y. Chen, J. Li, X. Zhang, Mater. Lett. 68 (2012) 435–438.
[16] Y. Song, S. Zhang, J. Li, C. Zhao, X. Zhang, Acta Biomater. 6 (2010) 1736–1742.
[17] J. Li, Y. Song, S. Zhang, C. Zhao, F. Zhang, X. Zhang, L. Cao, Q. Fan, T. Tang, Biomaterials 31 (2010) 5782–5788.
[18] M. Bohner, J. Lemaitre, Biomaterials 30 (2009) 2175–2179.
[19] X. Qiu, P. Wan, L. Tan, X. Fan, K. Yang, Mater. Sci. Eng. C 36 (2014) 65–76.
[20] F. Rahimi, B.T. Maurer, M.G. Enzweiler, J. Foot Ankle Surg. 36 (1997) 192–203.
[21] Y. Chen, Y. Song, S. Zhang, J. Li, C. Zhao, X. Zhang, Biomed. Mater. 6 (2011) 25005.
[22] A. Oyane, H.M. Kim, T. Furuya, T. Kokubo, T. Miyazaki, T. Nakamura, J. Biomed. Mater. Res. A 65A (2003) 188–195.
[23] R.Z. LeGeros, Clin. Orthop. Relat. Res. 395 (2002) 81–98.